

Phase Structure and Instability Problem in Color Superconductivity

Kenji Fukushima

RIKEN BNL Research Center, Brookhaven National Laboratory, Upton, New York 11973, USA

Received: date / Revised version: date

Abstract. We address the phase structure of color superconducting quark matter at high quark density. Under the electric and color neutrality conditions there appear various phases as a result of the Fermi surface mismatch among different quark flavors induced by finite strange quark mass; the color-flavor locked (CFL) phase where quarks are all energy gapped, the u -quark superconducting (uSC) phase where u -quarks are paired with either d - or s -quarks, the d -quark superconducting (dSC) phase that is the d -quark analogue of the uSC phase, the two-flavor superconducting (2SC) phase where u - and d -quarks are paired, and the unpaired quark matter (UQM) that is normal quark matter without pairing. Besides these possibilities, when the Fermi surface mismatch is large enough to surpass the gap energy, the gapless superconducting phases are expected. We focus our discussion on the chromomagnetic instability problem related to the gapless CFL (gCFL) onset and explore the instability regions on the phase diagram as a function of the temperature and the quark chemical potential. We sketch how to reach stable physical states inside the instability regions.

PACS. 12.38.-t Quantum chromodynamics – 12.38.Aw General properties of QCD

1 Family of color superconducting phases

The phase structure of matter composed of quarks and gluons described by Quantum Chromodynamics (QCD) has been investigated for many years, and in the high temperature and low baryon (or quark if deconfined) density region which is accessible in heavy-ion collisions interesting discoveries have been reported both in theories and in experiments. In the high density and low temperature region, on the other hand, our knowledge is still poor as compared with the rich physics expected in this region. Heavy-ion collisions are not suitable for the purpose to probe dense and cold quark matter, and such a system could be realized, if any, only in the cores of compact stellar objects. The experimental data from the universe is, however, quite limited and there is no smoking-gun for color superconductivity so far. Nevertheless, the theoretical challenge to explore the QCD phase structure is of great interest on its own. Also it would be potentially important in studying the structure and evolution of neutron stars.

In order to look into a dense quark system, some of concepts known in condensed matter physics have been imported into QCD in hope of analogous phenomena taking place. In this sense the physics of dense quark matter is, so to speak, “condensed matter physics of QCD” as articulated clearly in the review [1]. Superconductivity is definitely one of them. In general the Cooper instability inevitably occurs wherever there are a sharp Fermi surface

below which particles are degenerated and an attractive interaction between particles on the Fermi surface. Even QCD matter is not an exception and the condensation of quark Cooper pairs leads to color superconductivity.

A major difference between ordinary electric superconductivity in metals and color superconductivity in quark matter arises from the fact that quarks have three colors and three flavors in addition to spin, so that quark matter allows for many pairing patterns. The color and flavor degrees of freedom make the dense QCD phase structure so complicated that subtleties still remain veiled. In this article we shall argue what has been clarified by now and what should be solved in the future mainly following the discussions in my recent papers [2, 3].

1.1 Pairing patterns

Many theoretical works have revealed that the predominant pairing pattern is anti-symmetric in spin (spin zero), anti-symmetric in color (color triplet), and anti-symmetric in flavor (flavor triplet). Moreover, the color-flavor locking is known to be favored in energy, so that the color and flavor indices are locked together. Then there are three independent diquark condensates or gap parameters [4];

$$\langle \psi_i^a C \gamma_5 \psi_j^b \rangle \sim \Delta_1 \epsilon^{ab1} \epsilon_{ij1} + \Delta_2 \epsilon^{abs} \epsilon_{ij2} + \Delta_3 \epsilon^{ab3} \epsilon_{ij3}, \quad (1)$$

where (i, j) and (a, b) represent the flavor indices (u, d, s) and the color triplet indices (red, green, blue) respectively.

Gap Parameters	Phase
$\Delta_1 \neq 0, \Delta_2 \neq 0, \Delta_3 \neq 0$	CFL
$\Delta_1 = 0, \Delta_2 \neq 0, \Delta_3 \neq 0$	uSC
$\Delta_1 \neq 0, \Delta_2 = 0, \Delta_3 \neq 0$	dSC
$\Delta_1 = \Delta_2 = 0, \Delta_3 \neq 0$	2SC
$\Delta_1 = \Delta_2 = \Delta_3 = 0$	UQM

Table 1. A family of color superconducting phases; the color-flavor locked (CFL) phase, the u -quark superconducting (uSC) phase, the d -quark superconducting (dSC) phase, and the two-flavor superconducting (2SC) phase. UQM is unpaired quark matter. The sSC, 2SCsu, and 2SCds phases would not appear in the QCD phase diagram.

The charge conjugation C and the Dirac matrix γ_5 are required to make (1) a Lorenz scalar. Of course you can consider other kind of pairing between quarks which are totally anti-symmetric under exchange, and even different types of condensates may coexist. Actually diquark condensates such as spin-zero pairing in the color symmetric (color sextet) channel and spin-one pairing between quarks of the same flavor have been analyzed quantitatively [5, 6, 7, 8] and known to be much smaller than the predominant condensate. In this article we shall simply neglect them.

Under the pairing ansatz (1), Δ_1 is a gap parameter for the Cooper pairing between d and s flavors and green and blue colors. That is, Δ_1 is for bd - gs and gd - bs quarks and Δ_2 and Δ_3 are to be understood likewise;

$$\begin{array}{lll} \Delta_1 & bd\text{-}gs & gd\text{-}bs \\ \Delta_2 & rs\text{-}bu & bs\text{-}ru \\ \Delta_3 & gu\text{-}rd & ru\text{-}gd \end{array}$$

Each gap parameter is either zero or finite and there are $2^3 = 8$ combinations accordingly. Only five of eight phase possibilities as listed in Table 1 are of our interest relevant to the QCD phase diagram. When three gap parameters are all nonzero, this state is called the color-flavor locked (CFL) phase. When only Δ_1 is zero, this is the u -quark superconducting (uSC) phase named after the fact that remaining Δ_2 and Δ_3 are gap parameters for pairing involving u -quarks. The d -quark superconducting (dSC) phase is understood in the same way. The two-flavor superconducting (2SC) phase has only Δ_3 which is non-vanishing. The question is; where and how they show up on the phase diagram. The next section is devoted to this issue.

It is worth mentioning that these phases can be characterized by global symmetry breaking patterns. In particular the second-order phase transitions between the CFL phase and the uSC or dSC phase belong to the universality class same as an $O(2)$ vector model [9]. In QCD, neither the sSC (s -quark superconducting), 2SCsu (2SC of s - and u -quarks), nor 2SCds (2SC of d - and s -quarks) phase is realized actually because any pairing containing massive s -quarks is disfavored by the Fermi surface mismatch energy. (The solution branch of the gap equations belonging

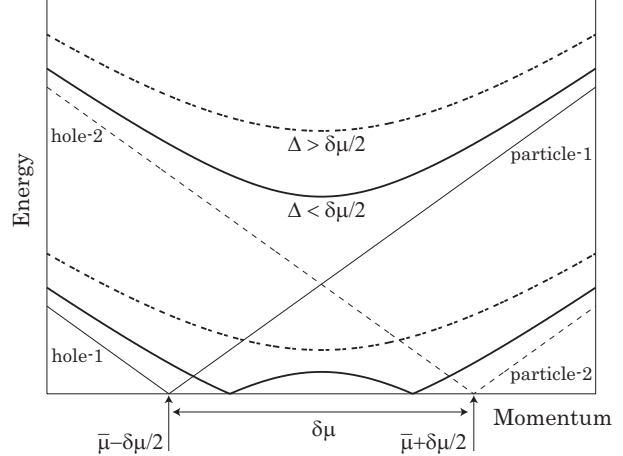


Fig. 1. The energy dispersion relations near the average Fermi surface $\bar{\mu}$ for 1 (solid lines) and 2 (dotted lines) species *without pairing* which have a Fermi surface mismatch $\delta\mu$. The dashed curves represent the energy dispersion relations *with pairing* between 1 and 2 species with the gap parameter $\Delta > \delta\mu/2$. When $\Delta < \delta\mu/2$ the dispersion relations cross zeros as shown by the solid curves and gapless quarks appear inside the blocking region.

to the 2SCsu phase has been examined in Refs. [10, 11] and confirmed to cost a larger energy.)

1.2 Gapless superconductors

The classification of superconducting phases under the pairing ansatz (1) is not complete until we will take account of the gapless superconducting states. They do not break any new symmetry and the phase transition to a gapless superconductor exists only at zero temperature [2]. In this sense the gapless CFL (gCFL) phase for instance which we will closely discuss later is not a totally new *phase* but can be regarded as a *variant* of the CFL phase augmented by the presence of gapless quarks. Before addressing the CFL problem, we shall see the simplest example that is actually enough for abstracting the essence.

Let us assume that there are two species of particles, 1 and 2, which have the Fermi momenta $\bar{\mu} - \delta\mu/2$ and $\bar{\mu} + \delta\mu/2$ respectively and they form a Cooper pair. The energy dispersion relations without pairing are shown by the solid and dotted lines in Fig. 1. In the presence of the 1-2 pair condensate Δ , the level repulsion by the energy Δ results in the dispersion relations which are smoothly connected between the hole state of 2 (or 1) and the particle state of 1 (or 2). In this simple model of superconductivity, therefore, the quasi-particle energy is expressed as

$$\epsilon^\pm(p) = \left| \sqrt{(p - \bar{\mu})^2 + \Delta^2} \pm \frac{1}{2}\delta\mu \right|. \quad (2)$$

As is obvious from Fig. 1 as well as from the expression (2), the dispersion relation comes to cross zeros when $|\frac{1}{2}\delta\mu| > \Delta$. The momentum region from one zero to another zero of the dispersion relation is called the block-

ing momentum region because the pairing within this region is hindered by degenerated particles. (In the case of Fig. 1 particle-2 is degenerated and particle-1 is absent in the blocking region.) Generally once a superconductor enters the gapless state, the gap parameter significantly decreases with increasing blocking momentum region.

In the language of physics, the condition for the gapless onset $|\frac{1}{2}\delta\mu| > \Delta$ means that a Cooper pair is not stable energetically. The pairing energy 2Δ is needed for breaking a Cooper pair into two particles and at the same time the mismatch energy $\delta\mu$ is released by doing so. If the mismatch is more expensive than the pairing, two particles would no longer form a Cooper pair. Roughly speaking, the realization of gapless superconductivity can be seen as a weak instability disrupting the Cooper pair only in a limited blocking region but not ruining the whole superconductivity.

We will end this subsection with one more remark. In this article (and in some literatures) $\delta\mu$ is frequently called the Fermi surface mismatch. It should be kept in mind that this mismatch is for the energy dispersion relations *without* pairing. In the presence of pairing, as observed in Fig. 1, the (approximate) Fermi surface is provided by the average $\bar{\mu}$. In other words two energy dispersions $\epsilon^\pm(p)$ in (2) have a common $\bar{\mu}$.

1.3 Strange quark mass effect and neutrality

We have so far illustrated what the gapless superconducting state is like. This gapless phase is often called the Sarma phase and was first demonstrated as a metastable state by Sarma [12]. The Sarma phase has recently attracted much interest since it was pointed out that it can be stable under the constraint to fix the particle number [13,14]. Also in the context of QCD the gapless 2SC (g2SC) phase first [15] and the gCFL phase next [16] have been shown to be stable under the electric and color neutrality conditions, that is; a potential *maximum* with respect to the gap parameters turns to be a *minimum* if additional gap parameter dependence through the neutrality conditions is properly taken into account. The gapless superconducting state stabilized in this way, however, turns out to be unstable after all, which is actually the main subject we shall argue spending the last half of this article.

Anyway, postponing the instability problem for a while, let us go on our discussion on the gCFL phase. Now we have to understand where $\delta\mu$ could come from. There are two distinct contributions from one origin; one is the direct M_s effect on the energy dispersion relations and the other is the induced M_s effect through the neutrality constraints.

The direct effect is simple. In the vicinity of the Fermi surface ($p \sim \mu$), the quark energy dispersion relation can be well approximated as

$$\sqrt{p^2 + M_s^2} - \mu \simeq p - \left(\mu - \frac{M_s^2}{2\mu} \right). \quad (3)$$

Thus the strange quark mass effect can be incorporated by a chemical potential shift proportional to M_s^2/μ . It is actually the case that the physics should change as a function of M_s^2/μ alone.

An explanation of the induced M_s effect needs some knowledge on the neutrality conditions. As far as a chunk of quark matter, like the cores of neutron stars which are of kilometer size, is concerned, neutrality with respect to charge associated with any gauge field must be required [17,18,19]. Besides, in the case of color charge in QCD, bulk quark matter must be a color singlet as a whole system. This is a more stringent condition than neutrality. The singletness is in principle to be implemented by an appropriate projection operator onto neutral states. There are many quarks in a macroscopic system and there are many thermodynamically equivalent states. If the number of singlet states grows in the large volume limit in the same way as the number of neutral states, the singletness condition can be simply ignored in thermodynamic properties. This is in fact the case in color superconducting quark matter [20]. Thus only the neutrality conditions for electric and color charges suffice for our purpose to explore the phase structure.

In the grand canonical ensemble, the number density of particles is specified by a chemical potential. We should introduce one chemical potential μ_e for the electromagnetic charge and eight chemical potentials μ_α for the color charges which are not gauge-invariant in non-abelian gauge theories. For the purpose of imposing neutrality it is enough to constrain only two eigenvalues of the color charge since zero charge remains to be zero charge if it is rotated by any gauge transformations. We thus only have to solve the color neutrality conditions with respect to two chemical potentials μ_3 and μ_8 [18].

Quark matter with three flavors would be automatically electric and color neutral if M_s is zero, meaning that μ_e , μ_3 , and μ_8 should be of order M_s^2/μ just like the direct M_s effect.

In summary, the direct and induced M_s effects are concisely expressed in a form of the effective chemical potentials for respective quarks with color a and flavor i as

$$\begin{aligned} \mu_{ai} = \mu - \mu_e(Q)_{ii} + \mu_3(T_3)_{aa} \\ + \mu_8(\frac{2}{3}T_8)_{aa} - (\mathbf{M}^2)_{ii}/2\mu, \end{aligned} \quad (4)$$

where $Q = \text{diag}(\frac{2}{3}, -\frac{1}{3}, -\frac{1}{3})$ and $\mathbf{M} = \text{diag}(0, 0, M_s)$ in flavor (u,d,s) space and $T_3 = \text{diag}(\frac{1}{2}, -\frac{1}{2}, 0)$ and $\frac{2}{\sqrt{3}}T_8 = \text{diag}(\frac{1}{3}, \frac{1}{3}, -\frac{2}{3})$ in color (red,green,blue) space. From (4) the Fermi surface mismatch for all the pairings is easily inferred; for the bd - gs pairing for instance the mismatch is

$$\delta\mu_{bd-gs} = \mu_{bd} - \mu_{gs} = \frac{1}{2}\mu_3 - \mu_8 + \frac{M_s^2}{2\mu}. \quad (5)$$

In the CFL phase at zero temperature a model-independent argument [18] yields $\mu_e = \mu_3 = 0$ and $\mu_8 = -M_s^2/2\mu$, and together with the above expression, the gapless onset condition (where gapless quarks begin appearing) is

$$\delta\mu_{bd-gs} = M_s^2/\mu > 2\Delta_1. \quad (6)$$

Numerical calculations in a model study [2,16] have confirmed this onset condition being a good estimate.

2 Phase diagram of dense quark matter

We will present the phase diagram first and then look closely at each phase in turn. Figure 2 is the phase diagram obtained in the Nambu–Jona-Lasinio (NJL) model. The model parameters are chosen as to yield $\Delta = 40$ MeV at $\mu = 500$ MeV and $M_s = T = 0$. The strange quark mass is fixed at $M_s = 150$ MeV which is the lowest estimate for the M_s effect in the intermediate density region. In Ref. [21] the authors solved the gap equations for the chiral condensates as well as the gap parameters and the chemical potentials. In the case of weak coupling, Δ is smaller and thus the critical value of the strange quark mass (or chemical potential) on the gCFL onset is smaller (or larger), and the gCFL phase is not substantially affected by the chiral dynamics then.

Even if the chiral condensate is not dealt with dynamically, a weird structure including a first-order phase boundary emerges on the phase diagram for large M_s^2/μ . As discussed in Ref. [2], however, the complicated structure seen at large M_s^2/μ is model and parameter dependent. Unfortunately there is no guiding principle to avoid unphysical artifacts in a certain parameter choice and one has to try and show all the cases for conclusive analyses [21]. In this article we dare not to touch that subtle issue and actually this is the reason why we present the phase diagram only for $\mu > 390$ MeV; a first-order phase boundary between the gCFL phase and the UQM is found at $\mu \simeq 388$ MeV.

The phase structure depicted in Fig. 2 is robust at least in a sense that the gross features would not be amended by assumptions we have made to draw this figure. Besides the chiral dynamics the important physics we have dropped is the K^0 -condensation that could delay the gapless onset [22] and the 't Hooft interaction term that embodies the instanton induced $U_A(1)$ breaking interaction in the NJL model Lagrangian. These two missing effects are actually closely linked. They could change the quantitative details of the phase diagram but no qualitative essence would be altered. We would not refer to the mixed phase possibility here, for it has already been settled [10].

We can see that in the lower density region near the gCFL phase the uSC region opens at finite temperature while the dSC phase is relevant at higher density. We can understand this behavior in a model-independent way and the existence of the “doubly critical point” is concluded [2]. In the subsequent subsections we shall discuss the important nature of the gCFL phase and how the uSC and dSC phases come out from the Fermi surface mismatch, and finally comment upon the doubly critical point.

2.1 gCFL phase

The gapless onset is located at $\mu \simeq 455$ MeV where $\Delta_1 = 24.9$ MeV and $\mu_8 = -24.7$ MeV and one can readily con-

firm that $\mu_8 \simeq -M_s^2/2\mu$ and $M_s^2/\mu \simeq 2\Delta_1$ as indicated by the condition (6). The gCFL phase has a definite meaning only at zero temperature because there is no clear distinction between gapless quarks and thermally excited quarks at finite temperature.

The onset condition (6) is only for *bd-gs* quarks with Δ_1 but gapless quarks can be present in another quark sector as well. In fact the energy dispersion relations of *rs-bu* quarks turn out to be identical to those of *bd-gs* quarks as long as the system remains to be in the CFL (not gCFL) phase. Thus *rs-bu* quarks become gapless at $M_s^2/\mu \simeq 2\Delta_2$ where $\Delta_2 = \Delta_1$ holds in the CFL phase. For larger M_s or smaller μ , the blocking momentum region in the *bd-gs* sector becomes wider, while the blocking region in the *rs-bu* sector is severely constrained by the neutrality conditions so that it must remain tiny (see Refs. [2,3,16] for details). As a result the *rs-bu* dispersion relations are kept to be almost quadratic in the entire gCFL region. Therefore only Δ_1 in the *bd-gs* quark sector significantly drops in the gCFL region due to the spreading blocking region with increasing M_s^2/μ .

Because this is an essential point in considering the instability problem later, we shall reiterate here;

bd-gs pairing with Δ_1 — gapless quarks appear at $M_s^2/\mu = 2\Delta_1$; the blocking region increases for larger M_s^2/μ .

rs-bu pairing with Δ_2 — gapless quarks appear at $M_s^2/\mu = 2\Delta_2$; the dispersion relations are kept to be almost quadratic in the entire gapless phase.

gu-rd pairing with Δ_3 — gapped quarks only.

ru-gd-bs pairing with all Δ 's — gapped quarks only.

2.2 uSC phase

The uSC phase results from the presence of the gCFL phase at zero temperature. In the gCFL phase, as explained in the last section, Δ_1 is significantly reduced than Δ_2 and Δ_3 . The pairing between *u-d* quarks is not reduced but Δ_3 is enhanced in the gCFL side as Δ_1 and Δ_2 decreases [2]. (Note that Δ_3 evaluated in the 2SC state is in general larger than Δ_3 in the CFL state for the same diquark interaction.) In this way the ordering $\Delta_1 < \Delta_2 < \Delta_3$ is realized.

It is a well-known fact that the critical temperature is of order of the gap parameter at zero temperature. We can anticipate that Δ_1 would melt first at finite temperature right above the gCFL region on the phase diagram. This means that the uSC phase where only Δ_1 is zero is expected when gCFL matter is heated. Figure 3 clearly shows that the phase structure is certainly as anticipated.

2.3 dSC phase

It is not the Fermi surface mismatch but the average Fermi momentum that is more relevant away from the gCFL region (see the expression (2) or Fig. 1). At zero temperature the average Fermi momenta are common in all the quark

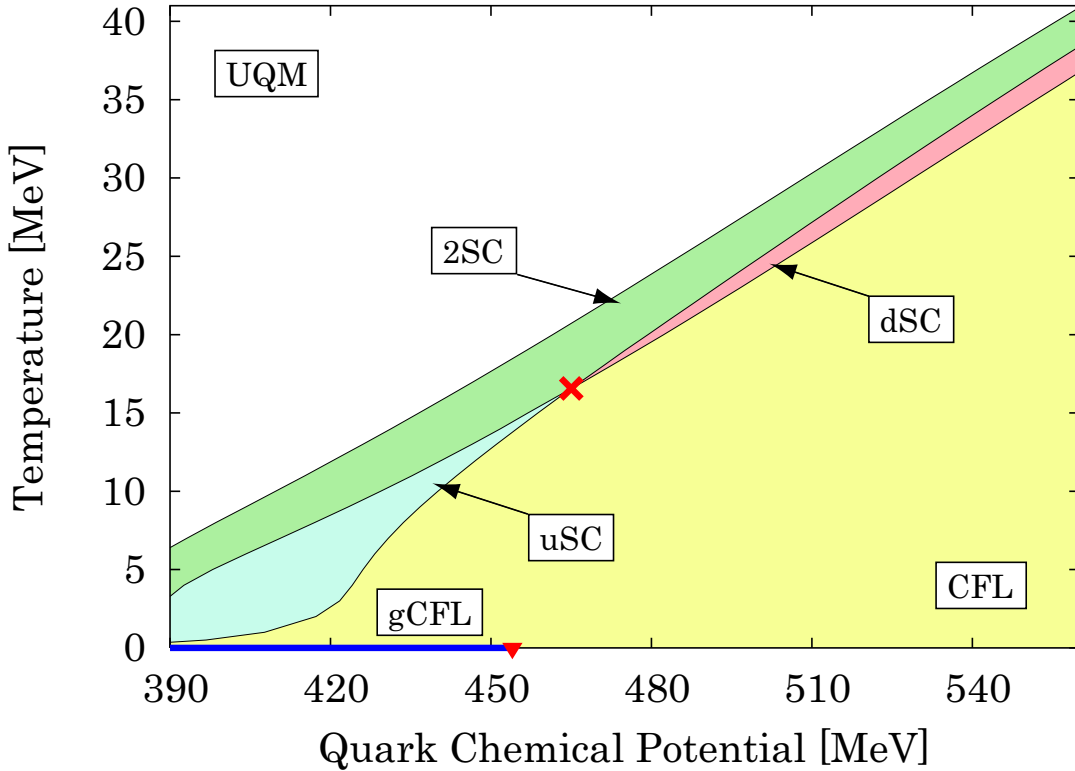


Fig. 2. Phase diagram of dense quark matter obtained in the NJL model with the parameters chosen to give $\Delta = 40$ MeV at $\mu = 500$ MeV and $T = M_s = 0$. The strange quark mass M_s is fixed at 150 MeV under the assumption that the first-order chiral phase transition occurred at some chemical potential below 390 MeV and $\langle \bar{s}s \rangle \propto M_s$ above that would not induce large corrections to M_s . The doubly critical point and the gCFL onset are marked by a cross and a triangle respectively.

sectors, that leads to equality in the number of nine (three colors and three flavors) quarks, and thus the electric and color neutrality is enforced [23].

The enforced neutrality at zero temperature is broken at small temperatures of a few MeV [2]. At higher temperature, especially in the vicinity of the critical temperatures, it is a good approximation to estimate μ 's in the normal phase, i.e., $\mu_e = -M_s^2/4\mu$ and $\mu_3 = \mu_8 = 0$. Then the ordering of the Fermi momenta, $\mu_s < \mu_u < \mu_d$ is concluded, which can be understood in an intuitive way; the number of s -quarks is suppressed by M_s and so d -quarks should be more abundant than s -quarks to maintain electric neutrality. From this, the average Fermi momenta should obey the following ordering; $\bar{\mu}_{su} < \bar{\mu}_{ds} < \bar{\mu}_{ud}$.

The gap equation to determine Δ 's contains the momentum integration around the Fermi surface which effectively picks up the density of states at the Fermi momentum. The larger the density of states is, the greater the gap parameter becomes. In this way the ordering $\Delta_2 < \Delta_1 < \Delta_3$ is realized from the average Fermi momenta ordering, which follows the presence of the dSC phase accordingly, as first discussed in Ref. [24].

2.4 Doubly critical point

The phase boundary on which Δ_1 goes to zero crosses the phase boundary on which Δ_2 goes to zero at the “doubly critical point” where two phase transitions with respect to Δ_1 and Δ_2 take place simultaneously. Since the existence of the uSC and dSC phases are robust and model-independent, so is the doubly critical point.

We would shortly comment upon a puzzling question concerning the doubly critical point. The question is the following; what are the effects of gauge field fluctuations on the doubly critical point?

In weak coupling the gauge field fluctuations bring about an induced first-order phase transition and the critical temperature is shifted [25, 26]. Between the CFL phase and the uSC or dSC phase, no manifest effects would be expected because eight gluons are all massive in both phases. Therefore we can conclude that the phase transitions from the CFL phase toward either the uSC or dSC phase is surely of second order belonging to the same universality class as an $O(2)$ vector model.

The gauge field fluctuations play an important role, on the other hand, between the 2SC phase and the uSC or dSC phase and the phase transition is forced to be of first order.

The doubly critical point is the point at which two phase transitions meet and three gluons become massless

around it since it faces the 2SC phase. This suggests that the phase transition must be of first order and the critical temperature should be shifted at the doubly critical point. But how is it possible if the phase boundaries facing the CFL phase are not shifted at all? Or, are they shifted near the doubly critical point by nearly massless gluons? To answer this question, further clarification on the treatment of the gauge field fluctuations is waited.

3 Chromomagnetic instability

The gapless superconductors could be stabilized by the neutrality conditions, at least, in the variational space spanned by gap parameters and chemical potentials, but after all, they have turned out to be unstable in a wider space including the gauge fields. The chromomagnetic instability signifies that the Meissner screening mass squared becomes negative, that is, the Meissner mass is imaginary. Before addressing the chromomagnetic instability problem first pointed out by Huang and Shovkovy [27] in the case of the g2SC phase and analyzed in Refs. [3, 28, 29] for the gCFL phase, we shall make a brief overview on the Debye and Meissner screening masses in the CFL phase, which would be useful to make a deeper insight into the instability problem. Our results are summarized in Fig. 3 and the goal of this section is to explain what is going on inside the instability regions presented by shadowed regions in this figure.

3.1 Debye and Meissner screening masses

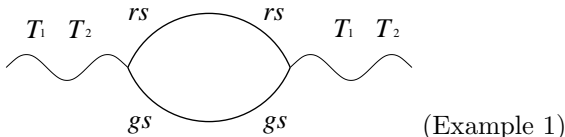
The Debye and Meissner screening masses are the screening masses for the longitudinal and transverse gauge fields respectively, which are defined by

$$m_{D,\alpha\beta}^2 = -\lim_{q\rightarrow 0} \Pi_{\alpha\beta}^{00}(\omega=0, \mathbf{q}), \quad (7)$$

$$m_{M,\alpha\beta}^2 = \frac{1}{2} \lim_{q\rightarrow 0} (\delta_{ij} - \hat{q}_i \hat{q}_j) \Pi_{\alpha\beta}^{ij}(\omega=0, \mathbf{q}), \quad (8)$$

where $\hat{q}_i = q_i/|\mathbf{q}|$ and $\Pi_{\alpha\beta}^{\mu\nu}$ is the polarization tensor for the gauge fields A_α^μ with the color and Lorenz indices denoted by α and μ . At high enough density the polarization tensor is dominated by the quark-loop contributions alone and so we shall neglect the gluon and ghost loops that would not depend on μ at the one-loop level.

Let us take one example to elaborate the quark-loop contributions for each gluon. The A_1 and A_2 gluons with the color indices labeled according to the Gell-Mann matrices in color space couple red quarks to green quarks and vice versa, while the flavor is not changed at any gluon vertices. For example, a diagram graphically shown as



can contribute to $\Pi_{11}^{\mu\nu}$ and $\Pi_{22}^{\mu\nu}$. Solid lines represent the quark propagator for rs and gs quarks in this specific case. From this kind of diagrammatic deliberation, it is easy to confirm that there is no mixing between gluons except A_3 - A_8 mixing. Moreover, some algebra can readily tell us that the screening masses are degenerate for the gluon pairs (A_1, A_2) , (A_4, A_5) , and (A_6, A_7) . In this article, like in Ref. [3], we shall denote $A_{1,2}$, $A_{4,5}$, and $A_{6,7}$ to mean either of the degenerated pairs.

3.2 Unstable channels and mixing with photon

If there is something funny in connection with gapless quarks in the quark-loop polarization like Example 1, it is expected to happen when both two quark propagators involve gapless energy dispersion relations. At the gapless onset, in fact, the quark-loop polarization consisting only of bd , gs , rs , and bu quarks is divergent, leading to the divergent contributions to the Debye and Meissner masses for $A_{1,2}$, A_3 , and A_8 gluons. You can easily check that the polarization diagrams relevant to the $A_{4,5}$ and $A_{6,7}$ gluon channels must have at least one of gu , rd , ru , bd , and bs quarks which are gapped.

It should be noted here about mixing between the A_γ photon and the A_3 and A_8 gluons. In the symmetric CFL phase with $M_s = 0$, there is no mixing with respect to A_3 , but in the present case with $M_s \neq 0$ and thus $\mu_e \neq 0$ in the gCFL phase, there is A_3 -mixing as well due to the isospin symmetry breaking. The mass squared matrix for A_γ , A_3 , and A_8 is a 3×3 matrix with nonvanishing off-diagonal components generating mixing. We will denote the eigenmodes of the mass squared matrix by \tilde{A}_γ , \tilde{A}_3 , and \tilde{A}_8 . The rotated photon represented by the \tilde{A}_γ field is massless all the way because the CFL and gCFL phases preserve a rotated electromagnetic U(1) symmetry. Once mixing occurs among A_γ , A_3 , and A_8 , it is simply a matter of convention which eigenmode should be identified as \tilde{A}_3 or \tilde{A}_8 . By this reason, though Figure 3 has the instability region with the label \tilde{A}_3 and \tilde{A}_8 , it does not mean that both of two eigenmodes suffer from the instability, but the fact is actually that only one of them does.

3.3 Divergences at the gCFL onset

The divergences in the Debye and Meissner screening masses at the gapless onset derive from the density of states which is divergent when the energy dispersion relations take a quadratic form; $\epsilon(p) \sim (p - \bar{\mu})^2/2\Delta$. That is, the density of states $n(p)$ is given by

$$n(p) = 4\pi p^2 \left[\frac{d\epsilon(p)}{dp} \right]^{-1} \quad (9)$$

and obviously $n(p) \rightarrow \infty$ when the slope of $\epsilon(p)$ is zero at $p = \bar{\mu}$.

The next question is whether the divergence is positive or negative in the Debye and Meissner masses. A

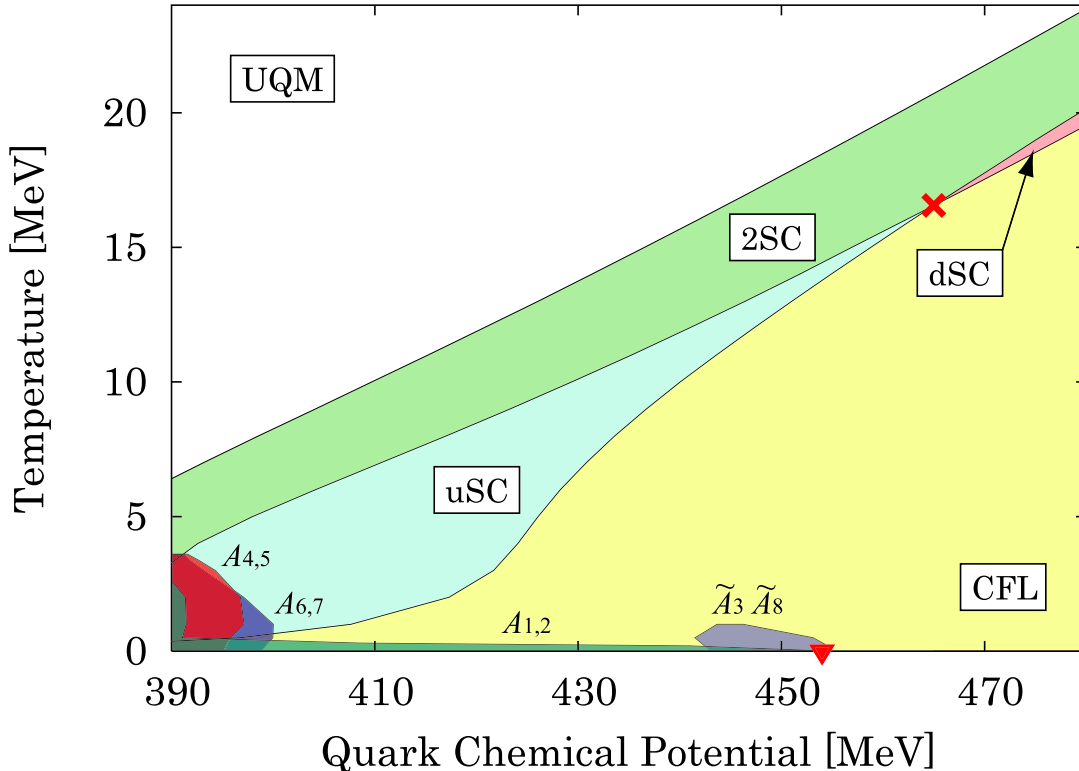
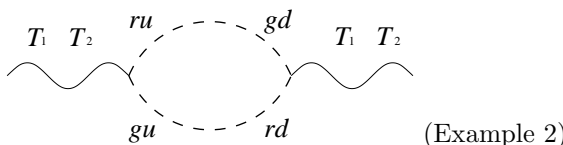


Fig. 3. A magnified drawing of the phase diagram around the gCFL and uSC phases with the instability regions overlaid.

naive intuition would be that both are positive, for in the CFL phase it is well established that $m_M^2 = \frac{1}{3}m_D^2$ should hold [9,30,31] and one might well consider that they are correlated in a similar way even in the presence of $M_s \neq 0$. This expectation is partly true but in an unexpected manner as we will shortly see below.

To find the relations between the Debye and Meissner masses, it is convenient to split the quark propagator into four distinct parts. If the quark mass effect is approximated as (3) near the Fermi surface, the energy projection operator divides the propagator into the *particle* part that is a function of $p - \bar{\mu}$ and the *antiparticle* part that is a function of $p + \bar{\mu}$. Moreover, in the Nambu-Gor'kov formalism, the quark propagator is a 2×2 matrix and its *diagonal* component is a normal propagation of particles, and its *off-diagonal* component is an abnormal propagation mediated by diquark condensates. There are thus four distinct combinations; diagonal-particle, diagonal-antiparticle, off-diagonal-particle, and off-diagonal-antiparticle.

The diagram shown in Example 1 is one example consisting of only the diagonal propagators. We can construct another example in the same gluon channel composed of only the off-diagonal propagators as follows;



where the upper propagator is the off-diagonal component proportional to Δ 's connecting ru and gd quarks, and the lower one is the off-diagonal component proportional to Δ_3 connecting gu and rd quarks.

It is important to note that the possible singular behavior originating from gapless quarks can reside only in the particle parts because antiparticles would never be gapless. The Debye mass squared receives the contributions only from particles which can be separated into the diagonal part, $[m_D^2]_{\text{diag}}$, and the off-diagonal part, $[m_D^2]_{\text{off}}$. The Meissner mass, on the other hand, has all of the particle-particle, particle-antiparticle, and antiparticle-antiparticle contributions. In Ref. [3] interesting relations have been found;

$$[m_M^2]_{\text{diag(pp)}} = -\frac{1}{3}[m_D^2]_{\text{diag}}, \quad (10)$$

$$[m_M^2]_{\text{off(pp)}} = \frac{1}{3}[m_D^2]_{\text{off}}, \quad (11)$$

where $[m_M^2]_{\text{diag(pp)}}$ is a part of the Meissner mass squared coming from the diagrams with two diagonal particle propagators (like Example 1) and $[m_M^2]_{\text{off(pp)}}$ with two off-diagonal particle propagators (like Example 2). The relation (10) might be strange at a glance, for we already know that $m_M^2 = \frac{1}{3}m_D^2$ in the CFL phase at $M_s = 0$. Then, how can we retrieve the relation $m_M^2 = \frac{1}{3}m_D^2$? Actually, as long as the system stays in the CFL side, the diagonal particle-antiparticle contribution $[m_M^2]_{\text{diag(pa)}}$ is *twice larger* than $[m_M^2]_{\text{diag(pp)}}$ and changes the overall sign in the relation between the Debye and Meissner masses. The other con-

tributions, $[m_M^2]_{\text{diag(aa)}}$, $[m_M^2]_{\text{off(pa)}}$, and $[m_M^2]_{\text{off(aa)}}$ are all negligibly small.

It might be surprising that these relations (10) and (11) are satisfied as they are even in the gCFL phase! The diagonal and off-diagonal parts both can generate divergent contributions at the gCFL onset. As far as the QCD problem is concerned, the diagonal contributions are always larger than the off-diagonal ones, leading to the Debye mass squared diverging *positively* and Meissner mass squared diverging *negatively* at the gCFL onset. The negative sign in (10) cannot be compensated in the gCFL phase since, unlike in the CFL phase, $[m_M^2]_{\text{diag(pa)}}$ is no longer a match for $[m_M^2]_{\text{diag(pp)}}$.

To put it in another way, the key relation (10) can be stated as follows: In the diagonal part, we can say that the particle-particle loops tend to induce *paramagnetism*, while *diamagnetism* stems from the particle-antiparticle loops. Usually in the superconducting phase, the diamagnetic tendency is greater enough to exhibit the Meissner effect. In gapless superconductors, however, antiparticles are never gapless and only the particle-particle loops are abnormally enhanced due to the presence of gapless quarks. As a result of that, the diamagnetism gives way to the chromomagnetic instability.

3.4 Away from the gCFL onset

Figure 3 shows the instability regions for respective gluons. The difference between the $A_{1,2}$ behavior and the \tilde{A}_3 - \tilde{A}_8 behavior can be understood from the difference between the *bd-gs* and *rs-bu* quark dispersion relations. It is only the diagram shown in Example 1 that causes singular behavior in $A_{1,2}$ around the gCFL onset. This diagram has two quark propagators; one of *gapless gs*-quarks and the other of *quadratic rs*-quarks. Since *rs* quarks are kept to be almost quadratic in the entire gCFL region, as we have explained before, the $A_{1,2}$ -instability extends over the whole gCFL region at small temperatures. The instability would not persist into regions at higher temperatures because the quadratic dispersion relations are easily affected by thermal excitations.

In contrast, the same species of quarks constitute the \tilde{A}_3 - \tilde{A}_8 instability region. The instability caused by two quadratic quark propagations lies in the entire gCFL region like the $A_{1,2}$ -instability but only at tiny temperatures of order eV. Instability boundaries at such low temperatures are not visible actually on the phase diagram. The instability caused by two gapless quark propagations is localized near the gCFL onset and spreads toward high temperatures than the $A_{1,2}$ -instability because it has nothing to do with quadratic quarks.

Although we would not go further into details, the Meissner screening masses evaluated in the g2SC phase [27] indicate that the \tilde{A}_8 -instability occurs starting at the g2SC onset and there also arises the instability for $A_{4,5,6,7}$ gluons whose boundary is found not at the g2SC onset but inside the 2SC region. In our results the $A_{4,5}$ and $A_{6,7}$ instability regions are located at large Fermi surface mis-

match and enter the uSC phase at higher temperature and then the 2SC phase farther. We conjecture that these instability regions for $A_{4,5}$ and $A_{6,7}$ would be linked to the instability found in the 2SC phase. The nature of the instability with respect to $A_{4,5}$ and $A_{6,7}$ is presumably different from the instability near the gCFL onset that we have seen in great details. In the aim of disclosing the QCD phase diagram in the intermediate density region, in particular, the $A_{4,5}$ and $A_{6,7}$ instability deserves further investigation.

4 Speculations

This final section is devoted to sketching some speculations on how to reach the stable states inside the instability regions on the phase diagram, which has been barely succeeded so far.

There are already some attempts to interpret and resolve the chromomagnetic instability problem [32, 33, 34, 35]. The most important among them is, in my opinion, the observation pointed out by Giannakis and Ren in Ref. [32] that the instability with respect to gluons can be interpreted as the instability toward a plane-wave crystalline superconducting phase.

The most straightforward interpretation of the chromomagnetic instability is, of course, spontaneous generation of the expectation value for the transverse gluons. The gauge field itself is, however, not a physical quantity depending on the gauge choice. Actually, what Giannakis and Ren realized in Ref. [32] is that the spontaneously generated gauge fields can be absorbed in the phase of the gap parameters by means of the gauge transformation. It should be noted that whether the gauge invariance is maintained or not does not matter. The gauge transformation in this manipulation simply means the change of variables.

The crystalline phase had been already studied [36] before the chromomagnetic instability was discovered. It is called the “crystalline” phase because the gap parameter takes a form of

$$\Delta(x) = |\Delta| e^{i\mathbf{q} \cdot \mathbf{x}}, \quad (12)$$

which breaks the translational and rotational invariance. The essential point is that there is another quark basis where the phase factor of (12) vanishes at the price of the vector potential arising in the effective action. Therefore, taking care of a vector potential turns out to be equivalent with dealing with the gap parameter with a phase factor corresponding to the given vector potential.

Let us rephrase the above mentioned idea in a slightly different way. Supposing we performed the derivative expansion of the thermodynamic potential $\Omega_A[\Delta(x)]$ which is now *gauged* with gluons, then we have in general,

$$\begin{aligned} \Omega_A[\Delta(x)] &\simeq \Omega_0[\Delta] \\ &- \kappa^{ab}[\Delta] \text{Tr}[(\partial_i + iA_i^*)\Delta^*(x)]^a [(\partial^i - iA^i)\Delta(x)]^b, \end{aligned} \quad (13)$$

where a and b represent the color triplet indices and $A^i = A_\alpha^i T^\alpha$ with the color adjoint index α . The average over \mathbf{x} is

symbolically implied in Tr . Then, an alternative definition of the Meissner screening mass is immediately available from this thermodynamic potential as

$$m_{M,\alpha\beta}^2 = \frac{1}{3} \sum_{i=1}^3 \frac{\partial^2 \Omega_A}{\partial A_\alpha^i \partial A_\beta^i} \Big|_{A=0} \sim 2\kappa^{ab} (T^\alpha)_{ca} (T^\beta)_{bd} \Delta^c \Delta^d, \quad (14)$$

where $\Delta(x)$ is assumed to be spatial constant. It might be instructive to see how this expression works actually. In the 2SC phase for example, $\Delta^a \propto \delta^{a3}$ and $(T^1)_{a3} = (T^2)_{a3} = (T^3)_{a3} = 0$, and hence one can instantly conclude that the A_1 , A_2 , and A_3 gluons are not Meissner screened. In the g2SC case the A_8 gluon is unstable, which can be stated by the condition $\kappa^{33} < 0$ because $m_{M,88}^2 \sim \kappa^{33}(\Delta^3)^2$.

Now we shall assume the crystalline superconducting phase with (12). The curvature of the thermodynamic potential with respect to \mathbf{q} is

$$\frac{1}{3} \sum_{i=1}^3 \frac{\partial^2 \Omega}{\partial q^i \partial q^i} \sim \kappa^{ab} \Delta^a \Delta^b. \quad (15)$$

In the 2SC phase the instability condition for \mathbf{q} to grow is given by $\kappa^{33} < 0$ again. This argument works well only in the (g)2SC case in which the A_8 -instability can be identified as the instability toward a crystalline superconducting phase equivalently. Essentially the above is what has been articulated in Refs. [32, 33].

The generalization to the (g)CFL problem is possible with a simple extension of the crystalline ansatz (12). As suggested by Giannakis and Ren, we can consider a *colored* crystalline superconducting phase with the gap parameter taking a form of

$$\Delta(x) = |\Delta| e^{iT^\alpha \mathbf{q}^\alpha \cdot \mathbf{x}}, \quad (16)$$

then it is almost obvious that the curvature with respect to \mathbf{q}^α is identical with the Meissner mass squared. In this sense, we can identify the instability regions in Fig. 3 with the colored crystalline phase with nonvanishing \mathbf{q}^α .

What we should do next is now apparent; \mathbf{q}^α are the new variational parameters to be determined so as to minimize the thermodynamic potential. This is a quite tough task, however. The number of the new variables is five corresponding to $A_{1,2}$, $A_{4,5}$, $A_{6,7}$, A_3 , and A_8 . To be worse, the rotational symmetry is broken by the direction of \mathbf{q}^α , and the momentum angle integration cannot simplify in evaluating the thermodynamic potential. So, the numerical calculations are too time-consuming to be done. Moreover it is difficult to achieve an enough accuracy to get reliable outputs in the multi-dimensional numerical integration. Maybe we have to abandon this apparent strategy and instead need to invent a wiser simplification that would not lose the important physics.

One possibility would be to go to the higher orders in the derivative expansion (13). The calculation would be feasible because the expansion coefficients can be evaluated at vanishing \mathbf{q}^α and the rotational symmetry is not broken then. Although we certainly have a chance to find

the energy minimum with some \mathbf{q}^α , there is no guarantee that the next higher order terms can be adequate to stabilize the potential. In any case this kind of calculation has yet to be performed.

Finally, if I am excused to speak of my own opinion, all these theoretical efforts will be tested in the lattice QCD simulation someday when the sign problem at finite density will be solved and the lattice spacing can be small enough to describe high density matter. The phase diagram like Fig. 3 is to be confirmed then.

This article is based on the talk given for the new talent sessions at International School of Subnuclear Physics 43rd Course held at Erice in Italy from Aug. 29 to Sep. 7 in 2005. I thank all the organizers for stimulating lectures and discussions at school.

References

1. K. Rajagopal and F. Wilczek, arXiv:hep-ph/0011333.
2. K. Fukushima, C. Kouvaris and K. Rajagopal, Phys. Rev. D **71** (2005) 034002 [arXiv:hep-ph/0408322].
3. K. Fukushima, Phys. Rev. D **72** (2005) 074002 [arXiv:hep-ph/0506080].
4. M. G. Alford, K. Rajagopal and F. Wilczek, Nucl. Phys. B **537** (1999) 443 [arXiv:hep-ph/9804403].
5. M. G. Alford, J. Berges and K. Rajagopal, Nucl. Phys. B **558** (1999) 219 [arXiv:hep-ph/9903502].
6. S. B. Ruster, I. A. Shovkovy and D. H. Rischke, Nucl. Phys. A **743** (2004) 127 [arXiv:hep-ph/0405170].
7. M. Iwasaki and T. Iwado, Phys. Lett. B **350** (1995) 163.
8. For a review on spin-one color superconductivity, see, A. Schmitt, arXiv:nucl-th/0405076.
9. K. Fukushima and K. Iida, Phys. Rev. D **71** (2005) 074011 [arXiv:hep-ph/0501276].
10. M. Alford, C. Kouvaris and K. Rajagopal, arXiv:hep-ph/0407257.
11. H. Abuki and T. Kunihiro, arXiv:hep-ph/0509172.
12. G. Sarma, J. Phys. Chem. Solids **24** (1963) 1029.
13. W. V. Liu and F. Wilczek, Phys. Rev. Lett. **90** (2003) 047002 [arXiv:cond-mat/0208052].
14. E. Zubkov, W. V. Liu and F. Wilczek, Phys. Rev. Lett. **91** (2003) 032001 [arXiv:hep-ph/0304016].
15. I. Shovkovy and M. Huang, Phys. Lett. B **564** (2003) 205 [arXiv:hep-ph/0302142]; Nucl. Phys. A **729** (2003) 835 [arXiv:hep-ph/0307273].
16. M. Alford, C. Kouvaris and K. Rajagopal, Phys. Rev. Lett. **92** (2004) 222001 [arXiv:hep-ph/0311286]; Phys. Rev. D **71** (2005) 054009 [arXiv:hep-ph/0406137].
17. K. Iida and G. Baym, Phys. Rev. D **63** (2001) 074018 [Erratum-ibid. D **66** (2002) 059903] [arXiv:hep-ph/0011229].
18. M. Alford and K. Rajagopal, JHEP **0206** (2002) 031 [arXiv:hep-ph/0204001].
19. A. W. Steiner, S. Reddy and M. Prakash, Phys. Rev. D **66** (2002) 094007 [arXiv:hep-ph/0205201].
20. P. Amore, M. C. Birse, J. A. McGovern and N. R. Walet, Phys. Rev. D **65** (2002) 074005 [arXiv:hep-ph/0110267].
21. H. Abuki, M. Kitazawa and T. Kunihiro, Phys. Lett. B **615** (2005) 102 [arXiv:hep-ph/0412382].
22. A. Kryjevski and T. Schafer, Phys. Lett. B **606** (2005) 52 [arXiv:hep-ph/0407329]; A. Kryjevski and D. Yamada, Phys. Rev. D **71** (2005) 014011 [arXiv:hep-ph/0407350].

23. K. Rajagopal and F. Wilczek, Phys. Rev. Lett. **86** (2001) 3492 [arXiv:hep-ph/0012039].
24. K. Iida, T. Matsuura, M. Tachibana and T. Hatsuda, Phys. Rev. Lett. **93** (2004) 132001 [arXiv:hep-ph/0312363].
25. T. Matsuura, K. Iida, T. Hatsuda and G. Baym, Phys. Rev. D **69** (2004) 074012 [arXiv:hep-ph/0312042].
26. I. Giannakis, D. f. Hou, H. c. Ren and D. H. Rischke, Phys. Rev. Lett. **93** (2004) 232301 [arXiv:hep-ph/0406031].
27. M. Huang and I. A. Shovkovy, Phys. Rev. D **70** (2004) 051501 [arXiv:hep-ph/0407049]; Phys. Rev. D **70** (2004) 094030 [arXiv:hep-ph/0408268].
28. R. Casalbuoni, R. Gatto, M. Mannarelli, G. Nardulli and M. Ruggieri, Phys. Lett. B **605** (2005) 362 [Erratum-ibid. B **615** (2005) 297] [arXiv:hep-ph/0410401].
29. M. Alford and Q. h. Wang, J. Phys. G **31** (2005) 719 [arXiv:hep-ph/0501078].
30. D. T. Son and M. A. Stephanov, Phys. Rev. D **61** (2000) 074012 [arXiv:hep-ph/9910491]; Phys. Rev. D **62** (2000) 059902 [arXiv:hep-ph/0004095].
31. D. H. Rischke, Phys. Rev. D **62** (2000) 054017 [arXiv:nucl-th/0003063].
32. I. Giannakis and H. C. Ren, Phys. Lett. B **611** (2005) 137 [arXiv:hep-ph/0412015]; Nucl. Phys. B **723** (2005) 255 [arXiv:hep-th/0504053].
33. M. Huang, arXiv:hep-ph/0504235.
34. D. K. Hong, arXiv:hep-ph/0506097.
35. M. Alford and Q. h. Wang, arXiv:hep-ph/0507269.
36. M. G. Alford, J. A. Bowers and K. Rajagopal, Phys. Rev. D **63**, 074016 (2001) [arXiv:hep-ph/0008208]; J. A. Bowers, J. Kundu, K. Rajagopal and E. Shuster, Phys. Rev. D **64**, 014024 (2001) [arXiv:hep-ph/0101067]; J. Kundu and K. Rajagopal, Phys. Rev. D **65**, 094022 (2002) [arXiv:hep-ph/0112206]; J. A. Bowers and K. Rajagopal, Phys. Rev. D **66**, 065002 (2002) [arXiv:hep-ph/0204079].